

Cite this: *Chem. Sci.*, 2019, 10, 6362

All publication charges for this article have been paid for by the Royal Society of Chemistry

Received 19th April 2019

Accepted 13th May 2019

DOI: 10.1039/c9sc01955c

rsc.li/chemical-science

# A reactive coordinatively saturated Mo(III) complex: exploiting the hemi-lability of tris(*tert*-butoxy)silanolate ligands†

Margherita Pucino,<sup>ID</sup> Florian Allouche,<sup>ID</sup> Christopher P. Gordon,<sup>ID</sup> Michael Wörle,<sup>ID</sup> Victor Mougel<sup>ID\*</sup> and Christophe Copéret<sup>ID\*</sup>

Coordinatively unsaturated Mo(III) complexes have been identified as highly reactive species able to activate dinitrogen without the need for a sacrificial reducing agent. Here, we report a coordinatively saturated octahedral Mo(III) complex stabilized by  $\kappa^2$ -tris(*tert*-butoxy)silanolate ligands, which is yet highly reactive towards dinitrogen and small molecules. The combined high stability and activity are ascribed to the dual binding mode of the tris(*tert*-butoxy)silanolate ligands that allow unlocking a coordination site in the presence of reactive small molecules to promote their activation at low temperatures.

## Introduction

The presence of a Mo center in the active site of the FeMo cofactor of nitrogenase enzymes has stimulated numerous studies on the synthesis of low valent Mo complexes and their reactivity towards small molecules.<sup>1</sup> Tri-coordinated complexes with bulky amide ligands like Mo[N(R)Ar]<sub>3</sub> (*R* = *t*Bu, Ar = 3,5-Me<sub>2</sub>C<sub>6</sub>H<sub>3</sub>) have been shown to be particularly reactive and able to cleave dinitrogen.<sup>2</sup> Such reactivity contrasts that observed for many mononuclear coordinatively saturated octahedral Mo(III) complexes, which are quite inert towards small molecules. To date, there are still a small number of examples<sup>3</sup> of tri-coordinated unsaturated Mo(III) compounds due to their propensity to form rather unreactive triply bonded Mo≡Mo dimers.<sup>4</sup> The use of bulky chelating ligands has thus been key to obtaining isolable, yet reactive coordinatively unsaturated Mo(III) centers.<sup>3,6,5</sup> This approach has enabled the synthesis of the first mononuclear Mo catalytic systems able to catalytically reduce N<sub>2</sub> to ammonia.<sup>6</sup>

The tris(*tert*-butoxy)silanolate (TBOS) ligand is not very sterically demanding but presents a variety of binding modes that allow for the formation of mono-nuclear complexes with a broad range of metals through coordination as a terminal  $\kappa^1$ , terminal  $\kappa^2$ , bridging  $\kappa^1\mu^2$  and bridging  $\kappa^2\mu^2$  ligand.<sup>7</sup> Terminal  $\kappa^1$  binding modes are observed for small metal ions such as trivalent Cr or Ga, while terminal  $\kappa^2$  modes are found for larger metal ions such as trivalent Sc, Yb, Lu<sup>8</sup> or Dy.<sup>9</sup> Mo(III) possesses an intermediate ionic radius between that of these two groups;

we thus reasoned that the TBOS ligands had the potential to stabilize Mo(III), while maintaining its reactivity towards small molecules, as such ligands can adopt different coordination modes and interconvert between them. Here, we present the synthesis and the reactivity of Mo(OSi(O*t*Bu)<sub>3</sub>)<sub>3</sub>, **1**, which displays a distorted octahedral geometry with three  $\kappa^2$ -TBOS ligands. Coordination of the TBOS ligand in a bidentate  $\kappa^2$ -fashion prevents dimerization and allows isolating a mono-nuclear Mo(III) complex, while the flexibility of its binding mode provides high reactivity as evidenced by the activation at low temperature of small molecules like N<sub>2</sub>, N<sub>2</sub>O and CO<sub>2</sub>, among others.

## Results and discussion

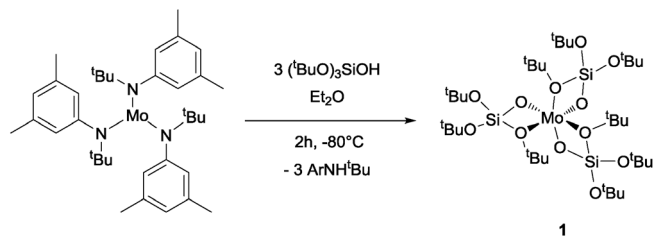
Mo(OSi(O*t*Bu)<sub>3</sub>)<sub>3</sub>, **1**, is prepared by reaction of [Mo(N(R)Ar)<sub>3</sub>] with (*t*BuO)<sub>3</sub>SiO-H (TBOS-H) in a slurry of diethyl ether at -80 °C; it is isolated as dark brown crystals in 36% yield after evacuation of the solvent and aniline byproduct under high vacuum at low temperature, followed by crystallization from pentane. NMR studies indicate a quantitative reaction, but the tedious isolation of this compound, which is required to separate the highly soluble compound **1** from the residual amine, diminishes the overall isolated yield for the pure crystalline form significantly. Compound **1** is, however, stable for months when in the solid state under an argon atmosphere at -35 °C and is rather stable in apolar solvents such as benzene, allowing investigation of its reactivity with small molecules in solution (Scheme 1).

Single-crystal X-ray diffraction<sup>10</sup> shows that complex **1** adopts a distorted octahedral geometry with three  $\kappa^2$ -TBOS ligands, where the Mo-O distance of the silanolate is *ca.* 0.3 Å shorter than that of the *tert*-butoxy moiety (2.020(4) Å vs. 2.302(4) Å) (Fig. 1). The <sup>1</sup>H NMR spectrum of **1** shows a single very broad

Department of Chemistry and Applied Biosciences, ETH Zurich, Vladimir-Prelog-Weg 2, 8093 Zurich, Switzerland. E-mail: ccoperet@ethz.ch; mougel@inorg.chem.ethz.ch

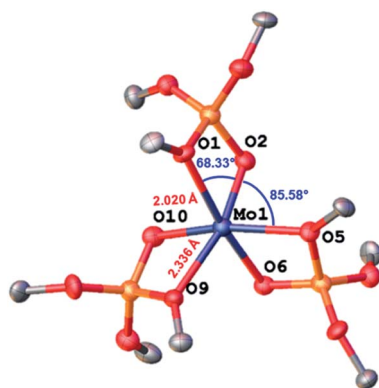
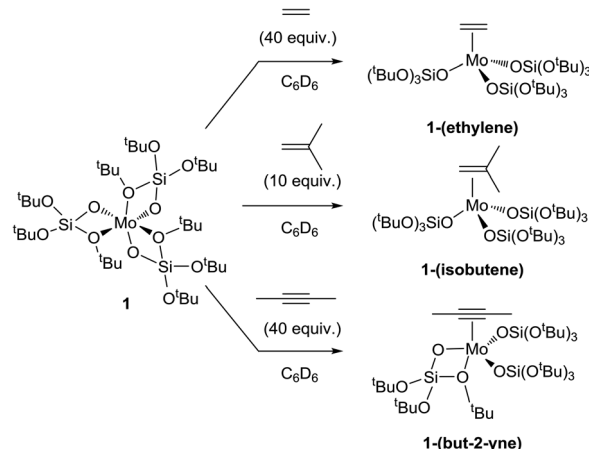
† Electronic supplementary information (ESI) available. CCDC 1826963–1826965, 1826967–1826969, 1826971–1826973. For ESI and crystallographic data in CIF or other electronic format see DOI: 10.1039/c9sc01955c



Scheme 1 Synthesis of  $[\text{Mo}(\text{TBOS})_3]$  (**1**).

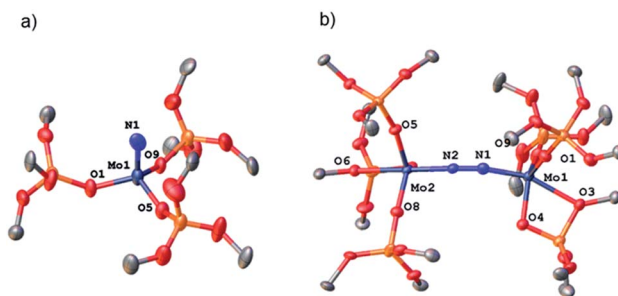
resonance at 3.82 ppm ( $\nu_2 = 164$  Hz, RT), suggesting a fluxional coordination of the *tert*-butoxy moieties in solution. At  $-80$  °C, the  $^1\text{H}$  NMR spectrum displays three peaks at 22.6, 4.9 and  $-1.36$  ppm, in agreement with the three inequivalent *tert*-butoxy groups (see the ESI† for details). However, complex **1** still displays broad peaks at this temperature, suggesting fast dynamics of the methyl groups. The magnetic susceptibility ( $\mu_{\text{eff}} = 3.74 \mu_{\text{B}}$ ) measured by the Evans method at 298 K is close to the expected value for a  $d^3$  complex with three unpaired electrons ( $3.75 \mu_{\text{B}}$ ).

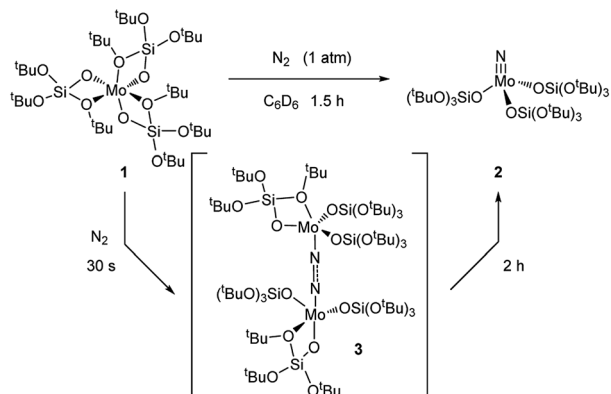
We first explored the reaction of complex **1** with alkenes (ethylene and isobutene) as well as alkynes (2-butyne). By condensing the gas at a low temperature ( $-196$  °C) in the solution and then warming to room temperature, the corresponding  $\pi$ -complexes were obtained in quantitative yields (Scheme 2, see the ESI† for details). The alkene and alkyne adducts  $[\text{Mo}(\text{C}_2\text{H}_4)(\text{OSi}(\text{OtBu})_3)_3]$ , **1-(ethylene)**,  $[\text{Mo}(\text{C}_4\text{H}_8)(\text{OSi}(\text{OtBu})_3)_3]$ , **1-(isobutene)**, and  $[\text{Mo}(\text{C}_4\text{H}_6)(\text{OSi}(\text{OtBu})_3)_3]$ , crystallize in a tetrahedral geometry, while **1-(but-2-yne)**<sup>11</sup> presents a square-based pyramidal one. In the latter, the  $\pi$ -accepting ligand occupies the apical site and three monodentate silanolate ligands are in the basal plane (XRD structures are presented in Fig. S11–13†). The significant lengthening of the C–C bond upon coordination (1.406(7), 1.391(9) and 1.283(5) Å for **1-(ethylene)**, **1-(isobutene)** and **1-(but-2-yne)**, respectively vs. 1.337(5) (ref. 12) 1.331(3) (ref. 13) and 1.202(5) (ref. 11) Å for the corresponding organic molecules) indicates a strong back-donation of the  $\text{Mo}(\text{III})$  center to these  $\pi$ -acid ligands.<sup>14,15</sup>

Fig. 1 Thermal ellipsoid plot at 50% probability of  $[\text{Mo}(\text{TBOS})_3]$  (**1**). Hydrogen atoms and siloxide methyl groups have been omitted for clarity.Scheme 2 Reaction of **1** with unsaturated hydrocarbons.

The fluxionality of the ligand prompted us to further investigate the reactivity of **1** towards small molecules, namely  $\text{N}_2$ ,  $\text{N}_2\text{O}$  and  $\text{CO}_2$ . Exposing **1** to a  $\text{N}_2$  atmosphere at room temperature led to an immediate color change from amber to dark blue within seconds. This blue color fades away after 2 h at room temperature, leaving a colorless solution.

Removal of all volatiles followed by extraction in pentane and crystallization at  $-35$  °C affords the  $\text{Mo}(\text{VI})$  nitride complex  $[\text{Mo}(\text{N})(\text{TBOS})_3]$ , **2**, in 40% yield. The relatively low isolated yield reflects the high solubility of the material, despite the quantitative reaction yield according to NMR. Single crystal X-ray analysis of **2** (Fig. 2a) shows a tetrahedral terminal nitride complex of  $\text{Mo}(\text{VI})$  with three  $\kappa_1$ -TBOS ligands (Scheme 3); the limited quality of the collected data however precludes an accurate discussion of bond distances. The presence of a nitride ligand was confirmed by FTIR, as evidenced by a band at  $1011 \text{ cm}^{-1}$  associated to  $\nu(\text{Mo}\equiv\text{N})$ .<sup>16</sup> To unequivocally verify the signal, we carried out the reaction with  $^{15}\text{N}_2$ . The infrared spectrum of  $^{15}\text{N}\equiv\text{Mo}(\text{TBOS})_3$  shows a band at  $997 \text{ cm}^{-1}$  that is red shifted compared to its  $^{14}\text{N}$  analogue, consistent with their attribution to  $\text{Mo}\equiv\text{N}$  vibration.  $^1\text{H}$  NMR of **2** shows a single and sharp peak at 1.49 ppm, in agreement with a  $\text{Mo}(\text{VI})$  diamagnetic species. The blue

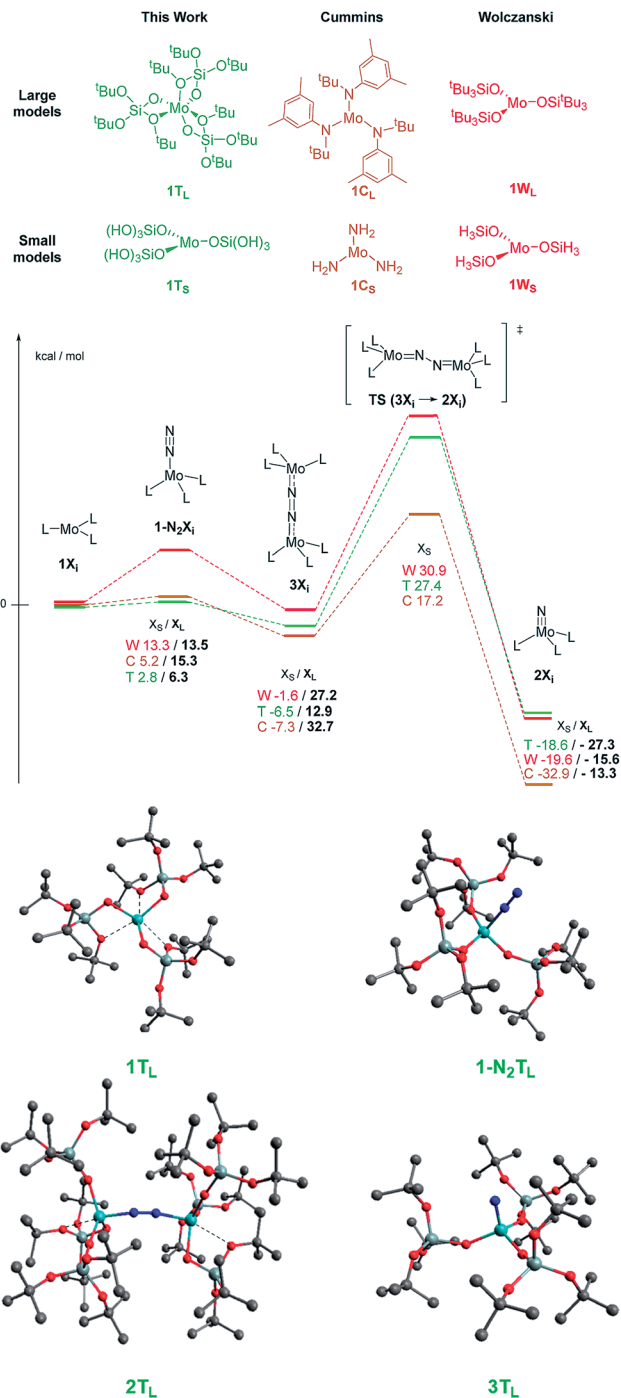
Fig. 2 Thermal ellipsoid plot at 50% probability of (a) **2** and (b) **3**. Hydrogen atoms, siloxide methyl groups and disorder have been omitted for clarity.



Scheme 3 Reaction of **1** with  $N_2$  yields  $[Mo(N)(TBOS)_3]$  (**2**) via a  $(\mu-N_2)[Mo(TBOS)_3]_2$  intermediate (**3**).

intermediate observed upon  $N_2$  addition can be isolated by rapid cooling of the reaction mixture ( $-196\text{ }^\circ\text{C}$ ) followed by fast solvent-exchange at  $5\text{ }^\circ\text{C}$  (from benzene- $d_6$  to pentane) and crystallization at  $-35\text{ }^\circ\text{C}$ . A dimeric Mo dinitrogen complex,  $(\mu-N_2)[Mo(TBOS)_3]_2$ , **3**, is isolated as dark blue crystals. Single crystal X-ray analysis of **3** (Fig. 2b) displays two Mo ions in a distorted TBP (Trigonal BiPyramidal) geometry with two  $\kappa^1$  and one  $\kappa^2$  TBOS ligands along with the end-on bound dinitrogen molecule sandwiched between the two Mo centers ( $Mo1-N1-N2$  and  $N1-N2-Mo2$  angles of  $172.5(3)^\circ$  and  $169.0(3)^\circ$ , respectively). The  $N1-N2$  distance is notably elongated with respect to the free  $N_2$  molecule ( $1.209(5)\text{ \AA}$  vs.  $1.0976(2)$  (ref. 11)  $\text{\AA}$ ) indicating a significant degree of activation. When **3** is warmed to room temperature the subsequent step of the overall  $6\text{ e}^-$  reduction of  $N_2$  occurs, leading to the formation of two equivalents of **2** (Scheme 3). While this mechanism is similar to the one observed with coordinatively unsaturated tris-amido complexes,<sup>17</sup> the complete process is much faster with **1** (2 h for the quantitative reaction at room temperature vs. less than 5% conversion after 12 h at  $28\text{ }^\circ\text{C}$  for  $Mo(NtBuAr)_3$ ).<sup>18</sup> It is worth noting that the corresponding complex bearing three very large siloxy ligands –  $Mo(OSitBu_3)_3$  – does not activate dinitrogen.<sup>5c</sup> This high reactivity towards  $N_2$  reduction is unusual for an octahedral  $Mo(III)$  complex, and highlights the particularity of the TBOS ligand, which can adopt mono- or bidentate binding modes while being relatively small compared to larger siloxy (*e.g.*  $tBu_3SiO$ )<sup>19</sup> or  $N(tBu)(3,5-Me_2C_6H_3)$  ligands.<sup>7g</sup>

To corroborate our data, we performed DFT calculations in order to better understand the reactivity difference between these three systems. Due to the very large size of the investigated systems, we calculated the entire potential free energy surface with simplified models<sup>20</sup> and calculated all reaction intermediates with the full ligand set (Scheme 4). The DFT calculations show that if electronic effects were the dominant factor (small models), one would predict the tris-amido system to be the most effective for  $N_2$  cleavage (TS energy of  $17.2\text{ kcal mol}^{-1}$  above separated reactants), while the siloxy derivatives should have significantly lower reactivity (with TS energies of  $27.4$  and  $30.9\text{ kcal mol}^{-1}$  for **1** and the model siloxy



Scheme 4 Top: calculated  $\Delta G$  in  $\text{kcal mol}^{-1}$  for the three compared systems  $1T_L$ ,  $2T_L$  and  $3T_L$ . Colored numbers refer to the small models and black numbers refer to the large ones. DFT models of complex **1** are in agreement with the XRD data, confirming the bond lengths and bond angles (calculated vs. experimental  $Mo-O1$   $2.410/2.302(4)$ ,  $Mo1-O6$   $2.043/2.046(4)$ ,  $Si-O1$   $1.707/1.677(5)$ ,  $O2-Mo-O1$   $67.2/68.33(16)$ ,  $O2-Mo1-O5$   $87.6/85.58(15)$ ), so are the other values for intermediate **c** and for the final nitride **e** (see the ESI† for details). Bottom: calculated structure for the large model of complex **1** for the reaction intermediates.

derivatives) in contrast with the observed trend, *i.e.* **1** reacts much faster with  $N_2$  than the Cummins  $Mo(III)$ , while the Wolczanski analog is unreactive towards  $N_2$  (Scheme 4).

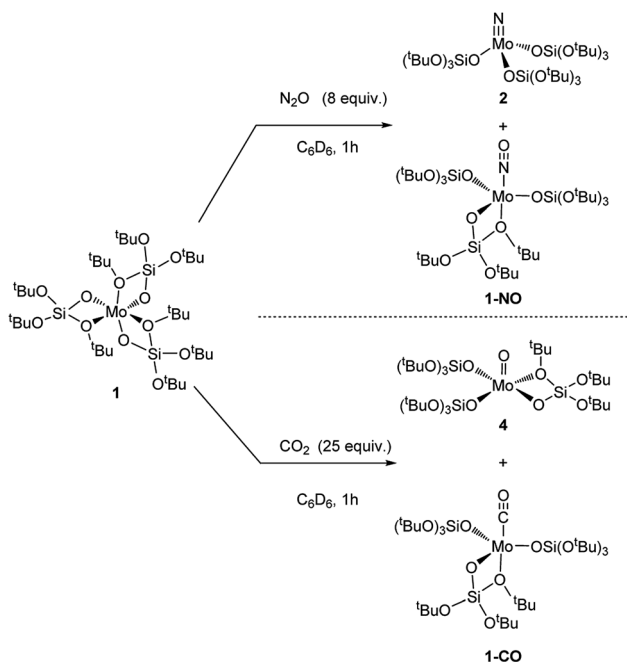


Once steric contributions are taken into consideration, it is notable how **1** yields more energetically accessible reaction intermediates and a significantly more stable nitrido complex: dinitrogen coordination costs only 6 kcal mol<sup>-1</sup> for **1** vs. 13–15 kcal mol<sup>-1</sup> for the two others, and the formation of the dimeric species prior to N<sub>2</sub> activation costs only 13 kcal mol<sup>-1</sup> for **1** vs. 27 and 33 kcal mol<sup>-1</sup> for the Cummins and Wolczanski systems, respectively, in line with their relative difference of reactivity. Overall, the DFT calculations show that the TBOS ligand favors N<sub>2</sub> activation because of its hemilability while protecting Mo(III) thanks to the possible κ<sup>2</sup>-configuration.

We then further explored the reactivity of **1** towards other small molecules. Upon exposure to N<sub>2</sub>O, a solution of **1** undergoes fast color change from amber to bright yellow upon warming up from liquid nitrogen temperature to room temperature (Scheme 4). Analysis of the reaction mixture by <sup>1</sup>H NMR shows the presence of two peaks at 1.51 and 1.50 ppm. FTIR analysis of this reaction mixture after removal of the solvent *in vacuo* reveals the presence of an intense band at 1678 cm<sup>-1</sup> which is attributed to Mo nitrosyl.<sup>16,21</sup> Two species are obtained as crystals, and X-ray crystallography analyses revealed species **2** and [Mo(NO)(TBOS)<sub>3</sub>], **1-NO** (Scheme 5). The nitrosyl compound **1-NO** crystallizes in a distorted TBP geometry, with a linear NO ligand (Mo–N–O = 178.6(2)°) in the apical position and a κ<sup>2</sup>-TBOS ligand. The Mo–NO bond distance of 1.715(3) Å is consistent with the literature value for linear nitrosyl complexes of Cummins and Zubietta, two molybdenum thiolate species with metal–nitrogen distances of 1.769(13) and 1.766(6) Å, respectively.<sup>21a,22</sup> It is slightly shorter, consistent with the weaker trans influence of the siloxy ligand. Despite a high kinetic barrier to reduction, the activation of N<sub>2</sub>O

has been observed with numerous low valent metal complexes.<sup>23</sup> However, the majority of metal-mediated activation of N<sub>2</sub>O generally involves the scission of the N–O bond, as the N–N bond is significantly stronger (~481 kJ mol<sup>-1</sup> and ~167 kJ mol<sup>-1</sup> for N–N and N–O, respectively) with a few examples of N–N bond activation,<sup>6a,21e,24</sup> highlighting the high azophilicity of the Mo complex **1**. The extremely challenging purification<sup>21a</sup> of the reaction mixture did not allow any further characterization of **1-NO** and of the impurities which appear to be paramagnetic.

Compound **1** when in contact with CO<sub>2</sub> also results in a rapid color change from amber to red upon warming from the liquid nitrogen temperature to room temperature, to yield a 1 : 1 ratio of two compounds according to NMR spectroscopy. Crystallization of the reaction mixture from pentane at –35 °C affords two sets of red crystals, assigned to [Mo(O)(TBOS)<sub>3</sub>], **4**, and [Mo(CO)(TBOS)<sub>3</sub>], **1-CO** (Fig. 3) according to X-ray single-crystal diffraction studies. The X-ray diffraction analysis of the monocarbonyl complex **1-CO** shows that the CO-adduct adopts a distorted TBP geometry with a κ<sup>2</sup>-TBOS ligand. The CO ligand occupies an axial position and is almost linear with a Mo–C–O angle of 175.2(3)°. The Mo–C and C–O distances of 1.931(3) Å and 1.156(3) Å, respectively, are in between those of Mo(CO)<sub>6</sub> (Mo–C 2.059(3) Å and C–O 1.125(5) Å)<sup>25</sup> and [Mo(CO)(Ph<sub>2</sub>PCH<sub>2</sub>CH<sub>2</sub>PPh<sub>2</sub>)<sub>2</sub>] (Mo–C 1.90(1) Å and C–O 1.19(1) Å)<sup>26</sup> indicating a π-back-donation on the carbonyl, comparable to that of *cis*-(diethylenetriamine)molybdenum tricarbonyl.<sup>27</sup> This is consistent with the red shift of the ν(C=O) band at 1869 cm<sup>-1</sup> observed in the FTIR spectrum, which can be attributed to the weak σ-donor ability of the TBOS ligand.<sup>28</sup> Complex **1-CO** can also be synthesized upon exposing **1** to an excess of carbon monoxide, see the ESI† for details. The structure of **4** presents a Mo(v) complex in a distorted TBP geometry with an equatorial oxo moiety with no trans ligand. The Mo=O bond length is 1.665(2) Å, which lies in the usual range for terminal Mo(v) oxo complexes.<sup>29</sup>



Scheme 5 Reaction of **1** with N<sub>2</sub>O and CO<sub>2</sub>.

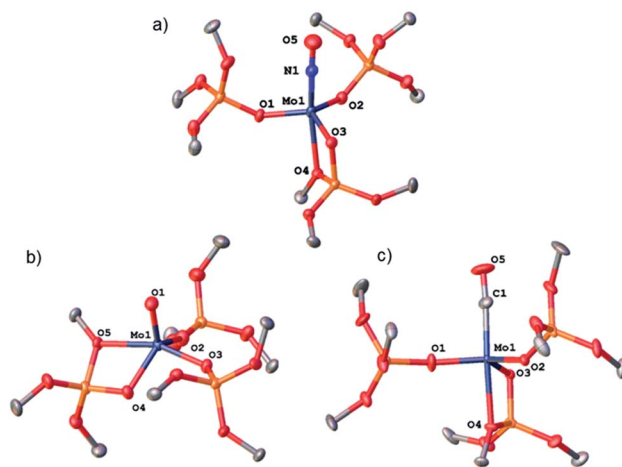


Fig. 3 Thermal ellipsoid plot at 50% probability of (a) **1-NO**, (b) **4** and (c) **1-CO**. Hydrogen atoms, siloxide methyl groups and disorder have been omitted for clarity.



## Conclusions

In conclusion, we have shown that the TBOS ligand can bind Mo(III) in a bidentate  $\kappa^2$ -fashion, providing an isolable – yet highly reactive – mononuclear octahedral Mo(III) complex. This complex thus activates a large variety of small – often rather inert – molecules, cleaving N–N and C–O bonds at low temperatures. An example is the 6-electron reduction of N<sub>2</sub>, which occurs faster than with other tri-coordinated Mo(III) complexes. The high reactivity of this coordinatively saturated complex illustrates the high adaptability of the TBOS ligand, which is able to protect highly reactive Mo(III) site from dimerization, without quenching its reactivity. The use of the TBOS ligand thus constitutes an alternative strategy to employ highly coordinatively unsaturated complexes towards small molecule activation at Mo centers.

## Conflicts of interest

There are no conflicts to declare.

## Acknowledgements

We acknowledge Dr Pavel Zhizhko for fruitful discussions. MP is thankful to the SNF (Swiss National Science Foundation) (200021\_169134). VM was supported by an ETH Zürich-Marie Curie action for people (FEL-08 12-2). CPG acknowledges the Scholarship Fund of the Swiss Chemical Industry. We thank Corinna Braghieri for help with the TOC graphic.

## Notes and references

- (a) D. C. K. V. Rajagopalan, E. Stiefel and W. E. Newton, *ACS Symp. Ser.*, 1993, **535**, 50–68; (b) M. Hidai and Y. Mizobe, *Chem. Rev.*, 1995, **95**, 1115–1133; (c) S. C. Lee and R. H. Holm, *Chem. Rev.*, 2004, **104**, 1135–1158.
- C. E. Laplaza and C. C. Cummins, *Science*, 1995, **268**, 861–863.
- (a) B. S. Buyuktas, M. O. Marilyn and P. Power, *Chem. Commun.*, 1998, 1689–1690; (b) C. C. Cummins, *Prog. Inorg. Chem.*, 1998, **47**, 685–836; (c) D. V. Yandulov, R. R. Schrock, A. L. Rheingold, C. Ceccarelli and W. M. Davis, *Inorg. Chem.*, 2003, **42**, 796–813; (d) D. V. Yandulov, R. R. Schrock, A. L. Rheingold, C. Ceccarelli and W. M. Davis, *Inorg. Chem.*, 2003, **42**, 796–813; (e) D. Kuiper, P. T. Wolczanski, E. B. Lobkovsky and T. Cundari, *J. Am. Chem. Soc.*, 2008, **130**, 12931–12943.
- F. A. Cotton, *Gen. Rev.*, 2005, 69–182.
- (a) K. Arashiba, Y. Miyake and Y. Nishibayashi, *Nature*, 2011, **3**, 120–125; (b) M. J. Bezdek, S. Guo and P. J. Chirik, *Inorg. Chem.*, 2016, **55**, 3117–3127; (c) D. S. Kuiper, P. T. Wolczanski, E. B. Lobkovsky and T. R. Cundari, *J. Am. Chem. Soc.*, 2008, **130**, 12931–12943.
- (a) D. V. Yandulov and R. R. Schrock, *Science*, 2003, **301**, 76–78; (b) L. A. Wickramasinghe, T. Ogawa, R. R. Schrock and P. Müller, *J. Am. Chem. Soc.*, 2017, **139**, 9132–9135.
- (a) K. L. Furdala and T. D. Tilley, *Chem. Mater.*, 2001, **13**, 1817–1827; (b) K. L. Furdala, I. J. Drake, A. T. Bell and T. D. Tilley, *J. Am. Chem. Soc.*, 2004, **126**, 10864–10866; (c) J. Jarupatrakorn and T. D. Tilley, *Dalton Trans.*, 2004, 2808–2813; (d) A. Fischbach, G. Eickerling, W. Scherer, E. Herdtweck and R. Anwender, *Synthesis and derivatization of homoleptic dinuclear lanthanide siloxide complexes*, 2004, vol. 59; (e) R. L. Brutchey, I. J. Drake, A. T. Bell and T. D. Tilley, *Chem. Commun.*, 2005, **29**, 3736–3738; (f) R. L. Brutchey, C. G. Lugmair, L. O. Schebaum and T. D. Tilley, *J. Catal.*, 2005, **229**, 72–84; (g) K. L. Furdala, R. L. Brutchey and T. D. Tilley, in *Surface and Interfacial Organometallic Chemistry and Catalysis*, ed., C. Copéret and B. Chaudret, Springer Berlin Heidelberg, Berlin, Heidelberg, 2005, pp. 69–115; (h) D. A. Ruddy, N. L. Ohler, A. T. Bell and T. D. Tilley, *J. Catal.*, 2006, **238**, 277–282; (i) M. Zimmermann, N. Å. Frøystein, A. Fischbach, P. Sirsch, H. M. Dietrich, K. W. Törnroos, E. Herdtweck and R. Anwender, *Chem.–Eur. J.*, 2007, **13**, 8784–8800; (j) V. Mougél, C. Camp, J. Pécaut, C. Copéret, L. Maron, C. E. Kefalidis and M. Mazzanti, *Angew. Chem., Int. Ed.*, 2012, **51**, 12280–12284; (k) M. P. Conley, M. F. Delley, G. Siddiqi, G. Lapadula, S. Norsic, V. Monteil, O. V. Safonova and C. Copéret, *Angew. Chem., Int. Ed.*, 2014, **53**, 1872–1876; (l) D. P. Estes, G. Siddiqi, F. Allouche, K. V. Kovtunov, O. V. Safonova, A. L. Trigub, I. V. Koptuyug and C. Copéret, *J. Am. Chem. Soc.*, 2016, **138**, 14987–14997; (m) F. Allouche, D. Klose, C. P. Gordon, A. Ashuiev, M. Wörle, V. Kalendra, V. Mougél, C. Copéret and G. Jeschke, *Angew. Chem., Int. Ed.*, 2018, **57**, 14533–14537.
- G. Lapadula, M. P. Conley, C. Copéret and R. A. Andersen, *Organometallics*, 2015, **34**, 2271–2277.
- F. Allouche, G. Lapadula, G. Siddiqi, W. W. Lukens, O. Maury, B. Le Guennic, F. Pointillart, J. Dreiser, V. Mougél, O. Cador and C. Copéret, *ACS Cent. Sci.*, 2017, **3**, 244–249.
- Experimental details for X-ray data crystal structure analysis collections of all complexes are given in ESI.† CCDC 1826972 (1), CCDC 1826973 (2), CCDC 1826967 (3), CCDC 1826964 (1-(ethylene)), CCDC 1826971 (1-(isobutene)), CCDC 1826963 (1-(but-2-yne)), CCDC 1826968 (1-NO), CCDC 1826969 (4), CCDC 1826965 (1-CO).
- (a) P. M. Boorman, M. Wang and M. Parvez, *Dalton Trans.*, 1996, 4533–4542; (b) E. Le Grogneq, R. Poli and P. Richard, *Dalton Trans.*, 2000, 1499–1506.
- H. J. Bowen, *Tables of interatomic distances and configuration in molecules and ions* The Chemical Society, Burlington House, London, 1958.
- L. Pauling and L. O. Brockway, *J. Am. Chem. Soc.*, 1937, **59**, 1223–1236.
- M. J. Byrnes, X. Dai, R. R. Schrock, A. S. Hock and P. Müller, *Organometallics*, 2005, **24**, 4437–4450.
- Reacting **1** with a large excess of 2-butyne (1000 equiv.) affords a gel, likely resulting from butyne polymerization.
- L. McAfee, *J. Chem. Educ.*, 2000, **77**, 1122.



- 17 J. J. Curley, T. R. Cook, S. Y. Reece, P. Müller and C. C. Cummins, *J. Am. Chem. Soc.*, 2008, **130**, 9394–9405.
- 18 C. E. Laplaza, M. J. A. Johnson, J. C. Peters, A. L. Odom, E. Kim, C. C. Cummins, G. N. George and I. J. Pickering, *J. Am. Chem. Soc.*, 1996, **118**, 8623–8638.
- 19 D. S. Kuiper, P. T. Wolczanski, E. B. Lobkovsky and T. R. Cundari, *Inorg. Chem.*, 2008, **47**, 10542–10553.
- 20 Q. Cui, D. G. Musaev, M. Svensson, S. Sieber and K. Morokuma, *J. Am. Chem. Soc.*, 1995, **117**, 12366–12367.
- 21 (a) T. Agapie, A. L. Odom and C. C. Cummins, *Inorg. Chem.*, 2000, **39**, 174–179; (b) J.-P. F. Cherry, A. R. Johnson, L. M. Baraldo, Y.-C. Tsai, C. C. Cummins, S. V. Kryatov, E. V. Rybak-Akimova, K. B. Capps, C. D. Hoff, C. M. Haar and S. P. Nolan, *J. Am. Chem. Soc.*, 2001, **123**, 7271–7286; (c) I. J. Blackmore, X. Jin and P. Legzdins, *Organometallics*, 2005, **24**, 4088–4098; (d) T. W. Hayton, P. Legzdins and W. B. Sharp, *Chem. Rev.*, 2002, **102**, 935–992; (e) C. E. Laplaza, A. L. Odom, W. M. Davis, C. C. Cummins and J. D. Protasiewicz, *J. Am. Chem. Soc.*, 1995, **117**, 4999–5000.
- 22 (a) A. Proust, P. Gouzerh and F. Robert, *Inorg. Chem.*, 1993, **32**, 5291–5298; (b) P. T. Bishop, J. R. Dilworth, J. Hutchinson and J. Zubieta, *Dalton Trans.*, 1986, 967–973.
- 23 W. B. Tolman, *Angew. Chem., Int. Ed.*, 2010, **49**, 1018–1024.
- 24 (a) M. E. Vol'pin and V. B. Shur, *Organomet. React.*, 1970, **1**, 55–117; (b) Y. Akio, G. Shigeo, O. Masaharu, T. Mitsuaki, I. Sakuji and K. Tominaga, *Bull. Chem. Soc. Jpn.*, 1972, **45**, 3110–3117; (c) W. H. Bernskoetter, E. Lobkovsky and P. J. Chirik, *J. Am. Chem. Soc.*, 2005, **127**, 14051–14061; (d) M. Falcone, L. Chatelain, R. Scopelliti, I. Živković and M. Mazzanti, *Nature*, 2017, **547**, 332–335.
- 25 C. W. Mak Thomas, *Z. Kristallogr. Cryst. Mater.*, 1984, **166**, 277.
- 26 M. Sato, T. Tatsumi, T. Kodama, M. Hidai, T. Uchida and Y. Uchida, *J. Am. Chem. Soc.*, 1978, **100**, 4447–4452.
- 27 F. A. Cotton and R. M. Wing, *Inorg. Chem.*, 1965, **4**, 314–317.
- 28 (a) V. Mougél and C. Coperet, *Chem. Sci.*, 2014, **5**, 2475–2481; (b) D. P. Estes, C. P. Gordon, A. Fedorov, W.-C. Liao, H. Ehrhorn, C. Bittner, M. L. Zier, D. Bockfeld, K. W. Chan, O. Eisenstein, C. Raynaud, M. Tamm and C. Coperet, *J. Am. Chem. Soc.*, 2017, **139**, 17597–17607.
- 29 (a) M. G. B. Drew and I. B. Tomkins, *J. Chem. Soc. A*, 1970, 22–25; (b) F. E. Inscore, H. K. Joshi, A. E. McElhaney and J. H. Enemark, *Inorg. Chim. Acta*, 2002, **331**, 246–256.

